WarmingUPGOO
Geothermie & Opslag Opschaling

Heat storage in salt caverns

Feasibility study – Twente use case

by

Mariëlle Koenen, Negar Khoshnevis Gargar and Dorien Dinkelman (TNO)

Mohamad Alameh (intern Utrecht University)

4 november 2025

Heat storage in salt caverns

Mariëlle Koenen, Negar Khoshnevis Gargar and Dorien Dinkelman (TNO), Mohamad Alameh (intern Utrecht University)
4 november 2025

Kwaliteitsborger(s)

Holger Cremer (TNO), Eva van der Voet (Ennatuurlijk Aardwarmte)

Summary

In the East of the Netherlands, aquifers suitable for Aquifer Thermal Energy Storage are scarce. However, these large scale heat storage systems can play a crucial role in the energy transition by providing flexibility to the energy system. Ennatuurlijk Aardwarmte is investigating how to increase the sustainability of their (expanding) heat network in the Twente area. They initiated this feasibility study for investigating the possibility of heat storage in underground salt caverns. Salt caverns are abundant in the Twente area (province Overijssel), as a result of salt mining. The caverns have flat, pancake-like shapes, in contrast to the salt dome caverns in the Northern part of the Netherlands. The concept of heat storage in salt caverns is partially similar to heat storage in aquifers with a hot and a cold well for injection and production within the same formation/cavern. The flow is reversed over the seasons. The key difference is in the flow dynamics in an open space filled with brine, compared to brine in a porous medium. COMSOL thermal simulations show that turbulent flow within the cavern results in quick mixing of the water and fast breakthrough at the producing well, both during loading and unloading. During loading, the amount of energy that can be added to the water declines as the temperature at the cold well increases. During unloading, the production temperature and hence the amount of heat that can be extracted decrease. For the Twente case study, a scenario was simulated for a flat, ellipse-shaped cavern with a volume of 226.195 m^3, loading for three months at 80°C (hot well), three months rest, and unloading for three months with a return temperature of 40°C (cold well). This resulted in 3 to 4 GWh of heat production, with an unloading temperature going down from ~60-65°C at the start, to 45°C at the end. The thermal efficiency is 28 to 47% for the first operational year, depending on whether pre-heating of the brine in the cavern was considered. In subsequent years, heat production could increase by several GWh (optimization highly recommended) as heat loss to the surrounding salt goes down, with thermal efficiencies expected to increase to ~75%. Even though these heat production estimates are only a fraction of the predicted heat demand of the Twente heat network in 2030 (~1.839 GWh), the performance of the salt cavern as storage technology is comparable to that of aquifer thermal energy storage systems. The simulated heat production, temperature levels and thermal efficiencies are comparable to the first operational years of the High Temperature ATES in Middenmeer, which is considered to be a successful storage system. It should be noted that, because of the turbulent flow in the cavern, the efficiency of such a system is likely more vulnerable to cavern dimensions, well position and loading and unloading conditions.
In addition to a positive thermal performance, a geomechanical simulation with DIANA showed that the cyclic charging of a salt cavern will not result in significant subsidence at surface level.
Next steps in a follow-up study would include techno-economic optimization of the design and operations for the Twente use case and evaluation of existing caverns (dimensions, well design etc) for re-use.

Contents

1 Introduction

Underground Thermal Energy Storage (UTES) technologies, including aquifer thermal energy storage (ATES), borehole thermal energy storage (BTES), and pit thermal energy storage (PTES), are key in managing seasonal heat demand and supply mismatches. In the Netherlands, ATES receives most attention as this technology can store large volumes of heat with relatively low impact at the surface. More important, it is applicable in various regions in the country (Dinkelman et al., 2020). In the eastern and south-eastern regions of the Netherlands, implementing an ATES system encounters difficulties because of the limited availability of appropriate aquifers, (Dinkelman et al., 2020). As a result, alternative storage methods must be explored. Ennatuurlijk (ENN), a Dutch energy company specializing in sustainable heating and cooling solutions, manages multiple district heating networks in the Twente region. They proposed investigating salt caverns for thermal energy storage, leveraging their abundance and potential in the eastern Netherlands. In the current study, the technical feasibility of heat storage in salt caverns from a subsurface point of view is investigated, with the focus on thermal efficiency and geomechanical safety of this technology. The geological characteristics, salt cavern dimensions in the Twente area and requirements for the specific heat networks of Ennatuurlijk form the basis of the study. The research is an extension of the study by Ekwadraat (2019), which concluded, based on energetic and economic (analytical) calculations, that heat storage could be economically feasible at the required scale. Additional research in the current study includes the flow dynamics within the cavern and its impact on thermal efficiency by numerical simulations, and geomechanical evaluation by geomechanical simulations.

This research is part of the WarmingUP GOO project, funded by MOOI (Missiegedreven Onderzoek, Ontwikkeling en Innovatie) for the built environment. This study aims to significantly contribute to the broader goal of sustainable energy transition and meeting ambitious climate objectives.

2 Twente use case

2.1 Heat network

The region of Twente, in the Province of Overijssel, is located in the East of the Netherlands at the border with Germany. There are about 600.000 inhabitants who live in 14 municipalities; half of them live in one of the three cities: Enschede, Hengelo, or Almelo.

Currently Twence provides high-temperature heat to more than 62.500 households and companies in Enschede through an underground heat pipeline. It has the ambition to provide high temperature heat to an additional 100.000 households in the remaining urban area in Twente. The most important heat sources for Hengelo and Enschede are waste heat from Twence (high-temperature heat, approximately 3600 TJ/yr) and Nobian (previously Nouryon) (low-temperature heat (40°C), approximately 100 MWth). Additional waste heat sources are available in the region and can be used in the future to enhance security of supply. For Almelo heat network, several low temperature sources are available.

Looking ahead to 2030, the forecasted total heat consumption for the area is estimated to reach nearly 17.500 TJ/yr of which 11.500 TJ/yr will be supplied via the regional heat network (ENN, personal communication). ENN and Firan operate the high and medium temperature district heating network in both Hengelo and Enschede, shown in Figure 1a. Figure 1b shows the location of salt caverns in relation to the heat network.
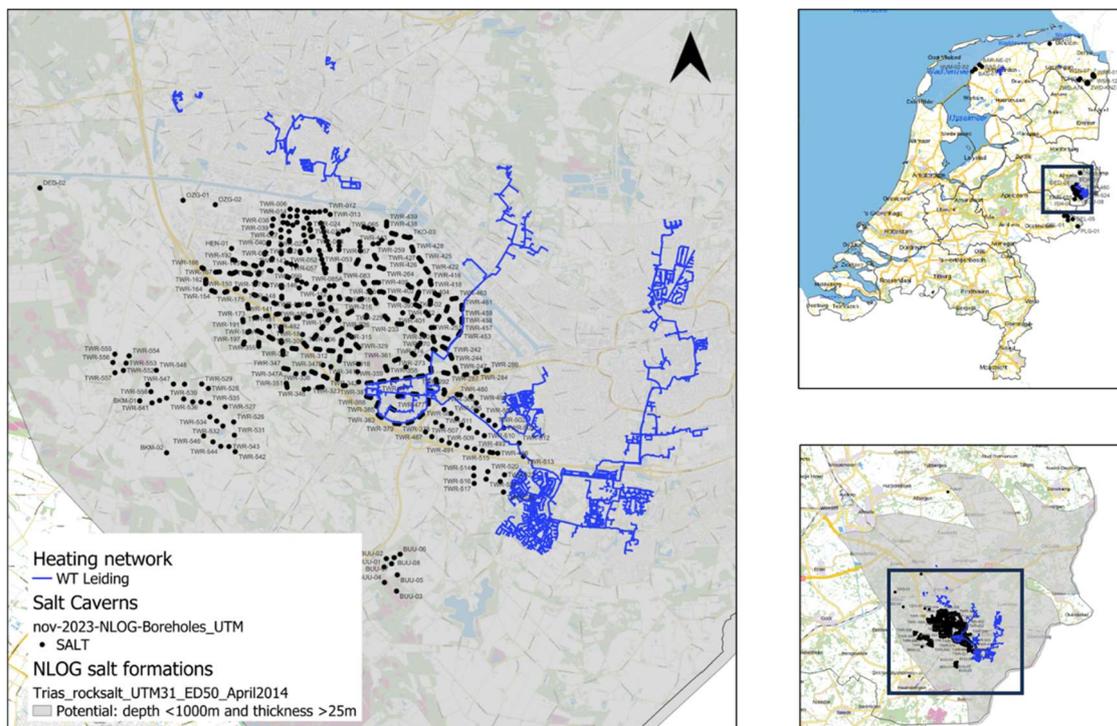

Figure 1. District heating network in Twente (blue lines) (created using Leiding_ENN_versie3 (arcgis.com) and location of salt caverns (black dots, from NLOG) in the region.

2.2   Geological setting and salt mining history

The subsurface geological structure in Eastern Twente comprises several distinct Formations, including the Solling Formation, Röt Formation, Muschelkalk Formation, Altena Group, Niedersachsen Group, and the North Sea Supergroup. The region is notably free of significant fault zones, facilitating the development of stable caverns. Salt is extracted from the Röt Formation with a flat stratigraphy in the east of the Netherlands. The Röt formation comprises layers A through D. Layer A stands out as the thickest and purest, while layers B, C, and D contain interspersed rock layers. Predominantly, layers A and B are thoroughly mined, with only a portion of layer C being utilized, ensuring the caverns' stability (Mollema, 2011).

Salt production in Twente is not a new practice, and it began in 1886 after unintentionally discovering a salt deposit during a well drilling for fresh water, which unexpectedly produced saltwater. Further explorations in 1909 revealed Zechstein Salt in Winterswijk and Rötsalt in Boekelo. By 1918, post-World War I, the Royal Dutch Salt Industry (KNZ) started extracting salt in Boekelo, initially from 325 meters deep. Later 1933, operations were moved to Hengelo, taking advantage of its closeness to the Twente Canal. The resulting salt caverns in the area are flat, and have a modest height of around 20 meters, depending on the location and salt layer thickness, and can extend up to 130 meters in diameter (Mollema, 2011). This in contrast with the salt caverns in northern Netherlands, where salt from dome-shaped structures several hundred meters tall but narrow in diameter.

Over time, salt extraction methods in Twente have significantly progressed, shifting from the conventional three-well setup to the innovative Single Cavern Completion (SCC) system in 2006 (Mollema, 2011). This modern system, facilitating injection and production via a single well, marked a substantial efficiency improvement.

Table 1 summarizes key details from some of the wells used for cavern production in the Twente area.

Table 1 Wells used for cavern production in the Twente area. Indicating the depth of the salt formation and the under- and overburden.

Well name	End-Date drilling	TVD [m]	Depth of Röt Evaporite Member	Thickness Röt Evaporite Member	Overlain by Formation	Underlain by Formation
TWR-487	29-11-07	472.0	389-471	82	Intermediate Röt Claystone Member	Soling Claystone Formation
TWR-504	02-02-10	486.5	404-485	81	Intermediate Röt Claystone Member	Soling Claystone Formation
TWR-360	14-09-89	463.5	394-463	69	Röt Claystone Member	Soling Claystone Formation
TWR-238	01-01-73	431.5	351-429	78	Soling Claystone Member	Soling Claystone Member
TWR-348	22-12-89	558.0	525-548	23	Röt Claystone Member	Soling Claystone Member
TWR-447	19-05-06	550.0	467-549	82	Röt Claystone Member	Soling Claystone Member
TWR-541	19-07-2017		462-544	82	Röt Claystone Member	Soling Claystone Member

2.3   Cavern development

Since the 1930s, the development of caverns in the Hengelo brine field has evolved due to advancements in leaching processes and technology. Initially, caverns, categorized as Single Completion Caverns (SCCs), were developed with a single well, reaching the top of the salt deposit and laterally expanding, forming hydraulic connections between neighboring caverns. In the 1960s and 1970s, Multi Completion Caverns (MCCs) were introduced, where multiple wells per cavern were drilled to enhance recovery by efficiently mining the salt between wells, particularly with blanket oil. The transition from category 2 to 3 introduced safety measures like a 5-meter safety roof and "inherently safe" caverns to prevent significant subsidence and sinkspaces. In the past decade, a single well has developed modern SCCs with a 5-meter safety roof and inherently safe concepts. This approach allows for better monitoring blanket oil levels, resulting in more effective cavern development than MCCs. Over time, newer caverns have been developed at increasing distances from the evaporation plant.

3 Heat storage in salt caverns

3.1 Operational concept

Salt caverns are created in the subsurface in the process of salt mining. At the end of the mining process, the cavern consists of an open space in the salt layer which is filled with brine to prevent the cavern from collapsing. For the purpose of heat storage in a salt cavern, the relatively cold (warm) brine from the cavern (open space in the salt layer) would be pumped to the surface through one (warm) well, heated through a heat exchanger, and back injected into the cavern through another (hot) well during the summer period (charging). Production of warm water from and injection of hot water into the single cavern thus occur simultaneously, which is necessary to keep the pressure within the cavern and prevent collapse of the walls. During the heat production (discharging) phase in winter, the flow is reversed and hot water is produced from the cavern through the hot well, the heat is extracted in the heat exchanger, and the warm water is back injected through the warm well. Again, production from and injection into the cavern occur simultaneously. The key difference with ATES is thus the storage of hot water in an open space rather than a porous medium. In addition, salt has different hydraulic and thermal properties compared to sand and clay. Physical processes are therefore significantly different. The next few sections explain which processes are relevant for storage in (salt) caverns.

3.2 Fluid flow and thermal processes

The thermal behavior of thermal storage systems and the surrounding rocks is primarily influenced by conduction and convection.

Convection involves the transfer of heat through the large-scale movement (flow) of a fluid. This heat transfer can be classified into two main types: The first type is forced convection, where fluid flow is driven by external forces. In the case of cavern heat storage, this involves the pumping of brine into and out of the cavern. The second type is free or natural convection, which occurs when fluid motion is caused by density differences. During heat storage, the density differences would be caused by the temperature difference between injected and produced water. When simulating flow of the brine into and out of the cavern, it is important to know if the flow is either laminar or turbulent. This is determined by the so called Reynolds number (Re), which is a dimensionless quantity used to predict flow regimes in fluid dynamics. It is calculated as the ratio of inertial forces to viscous forces in the fluid:

$$Re = \frac{Density \times Velocity \times Charactersti\ lengt}{Viscosity}$$

Interpretation of the Reynolds number:
- Re < 2000 indicates laminar flow.
- 2000 < Re < 4000 suggests transitional flow.
- Re > 4000 signifies turbulent flow.

Turbulent flow would enhance mixing of the water within the cavern, whereas laminar flow would limit mixing. Whether flow is predominantly turbulent or laminar in cavern heat storage needs to be calculated for each specific case.

Conduction is the process of transferring heat through a stationary material via physical contact. In turbulent flow, conductive heat transfer plays an important role in addition to convective heat transfer.

Conductive heat transfer also occurs where the brine is in contact with the salt at the walls of the cavern. Fourier's Law describes heat transfer by conduction in fluids and solids. The rate of heat conduction can be calculated by:

$$\frac{q_x}{A} = -k\frac{dt}{dx}$$

Where:
- q_x is the heat transfer rate in the x direction in watts [W]
- A is the cross-sectional area normal to the direction of flow of heat in [m^2],
- T is temperature in Kelvin [K]
- x is distance in [m]
- k is the thermal conductivity in $[W/(m*K)]$ in the SI system.

The quantity q_x/A is called the heat flux [W/m^2]. The quantity dT/dx is the temperature gradient in the x direction. For turbulent flow the thermal conductivity needs to be replaced by the effective thermal conductivity, which is the sum of thermal conductivity and turbulent thermal conductivity. For conduction at the boundary of the salt caverns, the thermal conductivity of the storage medium, salt in this case, is a key parameter. Parameters used in the simulations are given in Table 3.

Thermal stratification is a phenomenon in tank or cavern thermal energy storage (TES) systems where the storage medium develops distinct temperature layers, leading to a vertical separation of hot and cold regions. Most research has focused on heat storage in smaller scale tanks (i.e. Njoku et al., 2014; Bonanos and Votyakov, 2016; Karim et al., 2018), generally used for heat storage on daily or weekly basis, but the phenomenon has also been investigated for seasonal heat storage in rock caverns (Park et al., 2013). This natural layering effect is due to density differences caused by temperature variations, which cause hotter water to rise to the top and cooler water to sink to the bottom (buoyancy), creating a transition zone known as the thermocline. It is an effective way of improving the efficiency of thermal storage as the hot layer can be selectively extracted (Park et al., 2013). Several factors contribute to the formation and maintenance of thermal stratification in cavern storage.
1. The material properties of storage walls play a significant role, with TES systems using walls made of materials that have lower thermal diffusivity than the storage medium, thereby lowering the potential of natural convection and supporting stratification.
2. The temperature difference between the upper and lower layers whereby a larger temperature difference enhances the formation of distinct layers.
3. Lower flow rates.
4. The geometry of storage tanks, with the shape and dimensions of the storage container playing a pivotal role in establishing and maintaining stratification.
5. Location and design of inlet and outlet points.

3.3 Geomechanical processes

Several geomechanical processes, influenced by temperature and pressure, play a role during the production of rock salt from caverns. When storing thermal energy in aquifers, there will be frequent temperature (and pressure) changes in the cavern.

Salt creep is a typical process that can occur under pressure gradients in the subsurface. The process is highly dependent on temperature. The maximum pressure within the cavern (operating pressure) should not exceed the lithostatic pressure at any time, so that salt creep is directed into the cavern. Subsidence at surface level, related to salt creep as a result of cavern pressure below

lithostatic pressure, should remain within acceptable levels. In the absence of a clear criterium defined for the Netherlands the limit of 25 cm for the entire lifetime of a subsurface technology, as defined by the German Institute for Rock Mechanics (Susan, 2019), was chosen.

4 Simulation methodology

Thermal and geomechanical simulations were performed to assess system efficiencies and ground movement during cyclic thermal storage, tailored to the specific geological conditions and salt cavern dimensions in Twente. To investigate thermal evolution, heat losses and thermal efficiency of cavern storage systems, computational fluid dynamics (CFD) simulations and heat transfer modeling were performed using COMSOL Multiphysics. The geomechanical impact, i.e. pressure evolution in the subsurface surrounding the cavern and corresponding ground movement during cyclic heat storage in salt caverns is simulated using DIANA FEA software.

4.1 COMSOL simulations

The process of heat storage is simulated in four phases: storage (loading) and production (unloading) as illustrated in Figure 2, both followed by a rest phase. Initially, the cavern is filled with relatively cold (warm) brine. In the base base the initial brine temperature was set at 40°C rather than the natural background temperature (20°C), representing a case in which pre-heating takes place, or simulate conditions more representative from year 2 onwards. In a sensitivity analysis the first operational year without pre-heating is simulated. During the **loading phase** (Figure 2, left), brine is extracted from the cold well at the bottom of the cavern. Simultaneously the hot water is reinjected through the hot well at the top of the cavern. In the **unloading phase** (Figure 2, right), the flow direction is reversed. The heat stored in the cavern is extracted by producing brine from the hot well at the top of the cavern. The cooled brine is reinjected through the cold well at the bottom of the cavern.
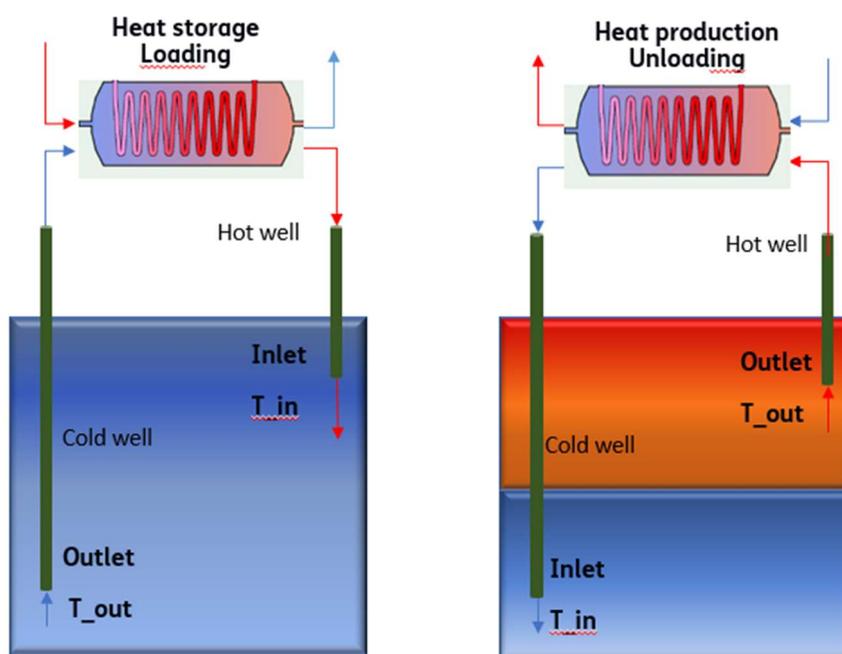

Figure 2. Schematic representation of loading and unloading phases applied in the thermal simulations. Note that the temperature conditions in the right image represent stratification which is not necessarily representative.
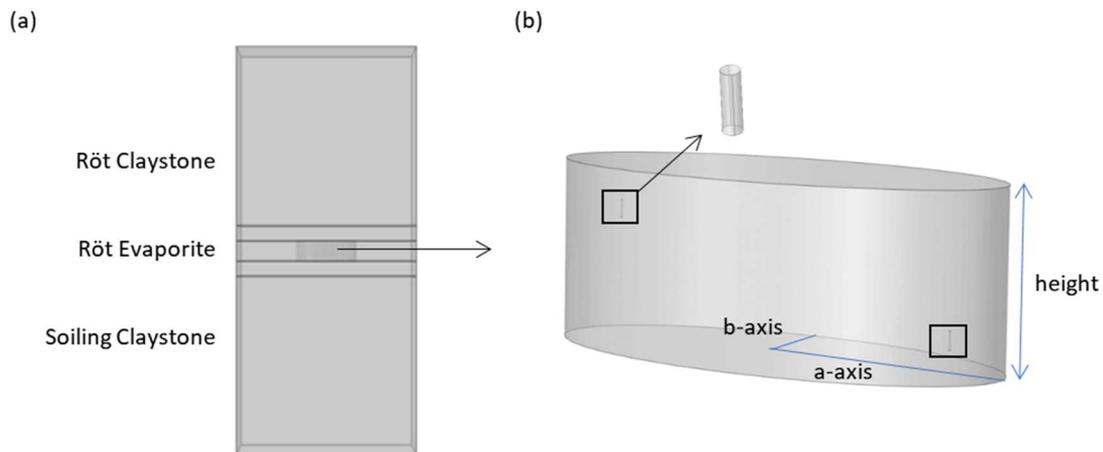
Figure 3. Representation of subsurface model with the salt cavern with (a) the entire model and (b) close up of the cavern and positions of the wells.

The subsurface model is based on the conditions in Twente. The modeled salt cavern is created within a 100 m thick Röt Evaporite layer, with 350 m of Röt Claystone above and 350 m of Solling Claystone below. The cavern is represented by an ellipse-shape with a major and minor axis of respectively 120 and 60 m and a thickness of 40 m. The cavern is located in the middle of the evaporite layer (Figure 3a). Initially, the temperature within the cavern is 20°C. The inlet and outlet points of the wells were strategically positioned within the cavern to obtain a high storage efficiency; the inlet and outlet are placed at a distance of 10m of the cavern's top and bottom, as well as from the sides (Figure 3b). Information on the mesh generation of the COMSOL model can be found in Appendix A. In the base case scenario, the storage temperature is 80°C and the return temperature is 40 °C. A theoretical operational scheme was applied with four phases each for 3-months: storage, rest, production, rest. It is assumed that the mass flow rate entering the system is equal to the mass flow rate exiting the system:

mass_{in} = mass_{out}.

1 phase = 3 months = 2160 h = 90 days

The volume of the ellipse-shaped cavern can be calculated using the formula:
$Volume = \pi \times a \times b \times h$
where:
- $a = 60\ m$ is the semi-major axis of the ellipse
- $b = 30$ m is the semi-minor axis
- $h = 40$ m is the height of the cylinder.

Volume= 226.195 m^3

In the base case simulation a flow rate of 48 kg/s was applied, in the sensitivity study this was decreased to 32 kg/s.

Based on the brine properties in

, it is safe to assume that the Reynolds number is >> 4000, and therefore the flow regime will be turbulent. The k-ε flow model is used, which is a Reynolds-Averaged Navier-Stokes (RANS) turbulence model. For heat transfer the Kays-Crawford heat transport turbulence model is applied. See COMSOL user guide for more details (The Heat Transfer Module User's Guide[1]).

4.2 DIANA simulations

Figure 4 shows the 2D axisymmetric model constructed in DIANA[2] for geomechanical simulations. The geometry and formation depths are mostly consistent with those used in the COMSOL Multiphysics simulations. A key difference is that in DIANA, the cavern is cylindrical rather than elliptical, to avoid potential edge effects that could arise in the DIANA simulation environment. The diameter is 60 m. A surface temperature of 10°C and a fixed geothermal gradient of 0.034°C/m were applied.
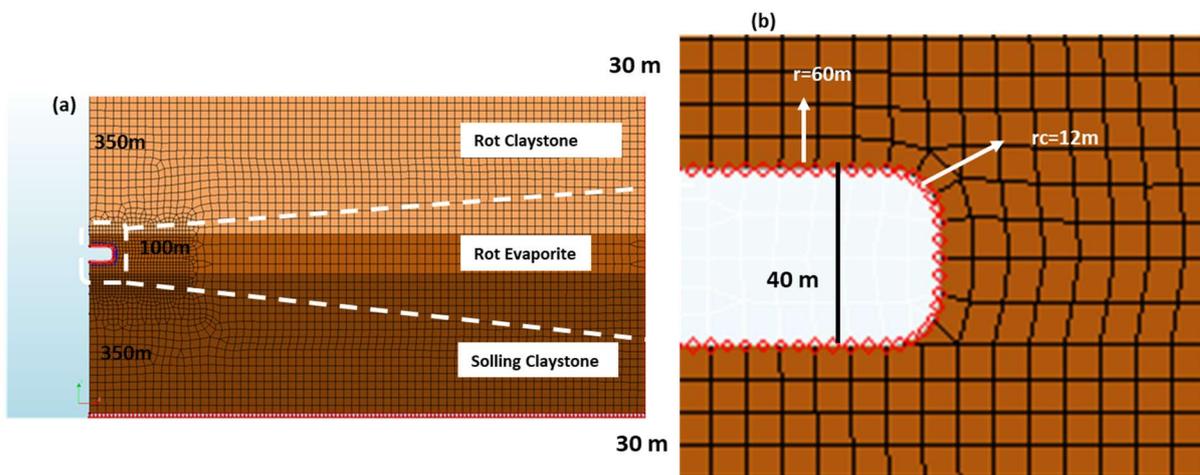

Figure 4. Geomechanical Model Setup in DIANA FEA. The mesh is refined near the cavern boundaries to accurately capture stress concentrations and deformation patterns within the surrounding rock formations.

For the model lifecycle set up, four phases are modelled (Table 2): (1) the cavern construction phase (1.5 years), where the cavern pressure is changed linearly in time from lithostatic to halmostatic, simulating leaching of the cavity; (2) the brine production phase (7.5 years), with constant hemostatic pressure (3) Rest phase in between end of brine production and start of storage operations (10 years) (4) the heat storage operations (10 years).

In a sensitivity study the storage and return temperature levels were changed.

Table 2. Operational lifecycle implemented in DIANA. * Base case scenario, the actual temperature within the cavern varies between 40 °C and 80 °C depending on the phase in the storage cycle

Lifecycle Phases Of The Salt Cavern	Start/End (days)	Cavern Pressure	Temperature (°C)
Cavern Construction	0-548	Lithostatic to Halmostatic	20
Brine production	548-3285	Halmostatic	20
Rest after production	3285-6937	Halmostatic	20
Heat storage cycles	6937-10537	Halmostatic	40/80*

---

[1] https://doc.comsol.com/5.4/doc/com.comsol.help.heat/HeatTransferModuleUsersGuide.pdf

[2] Home - DIANA

4.3   Rock parameters and brine properties

Table 3 gives an overview of the parameters used in the COMSOL and DIANA simulations. Salt properties have been based on literature or on properties for Zechstein salt, extracted from Hunfeld et al., 2022, since data for Röt Salt are not available.
Table 4 shows the geomechanical properties that are used in the simulations.

Table 3. Summary of rock properties used in the simulations.

Parameter	Unit
Evaporite density	2200 [kg/m³]
Evaporite Heat Capacity	909 [J/kg·K]
Evaporite Thermal Conductivity	6 [W/m·K]
Rot Clay Density	2000 [kg/m³]
Rot Clay Heat Capacity	1350 [J/kg·K]
Rot Clay Thermal Conductivity	2 [W/m·K]
Soling Clay Density	2600 [kg/m³]
Soling Clay Heat Capacity	1400 [J/kg·K]
Soling Clay Thermal Conductivity	1,2 [W/m·K]

Table 4. Summary of geomechanical properties for salt used in the simulations.

Parameter	Unit
Young's Modulus	30-32 [GPa]
Poisson's Ratio	0,26-0,3 [−]
Thermal Expansion Coefficient	3×10^{-5} [1/K]
Initial Stress Ratio [K_0]	1
Elastic Equivalent Young's Modulus [GPa]	0,075
Elastic Equivalent Poisson's Ratio [−]	0,005

5   Simulation results

5.1   Thermal evolution and efficiency

Figure 5 shows the thermal simulation results for temperature within the cavern at specific times for the base case scenario. In this scenario it is assumed that the initial temperature within the cavern is 40°C (i.e. preheating of cavern has taken place, although heat loss to surrounding salt was not considered). After 10 days of loading at 80 °C (Figure 5a) a clear temperature rise can be seen in the right half of the cavern. High temperatures up to the storage temperature can be seen around the inlet of the hot well. Quick mixing results in a slow but steady rise of the temperature in the entire cavern, without the process of thermal stratification, which was described in section 3.2, taking place. Also heating of surrounding salt is shown at the right half of the cavern. At the end of the loading phase, after 90 days of loading (Figure 5b), the heat seems to have mixed quite well with an average temperature of around 65°C, with higher temperatures only around the inlet of the hot well. Heating of surrounding salt is now visible around the entire cavern. At the end of unloading, after 90 days of rest and 90 days of unloading (figure c), the cavern has a (nearly) homogeneous temperature of around 45°C.

Figure 6 shows the temperature evolution at the hot and cold wells during loading, rest and unloading phases. The simulation clearly shows a fast breakthrough of the heat at the cold well during loading. At the end of the loading phase the temperature at the cold well is 65°C. During the rest phase the temperature around the inlet of the hot well goes down from 80°C to 65°C quickly, and this is also the temperature at the start of the unloading phase. At the end of unloading the production temperature is ~45°C.
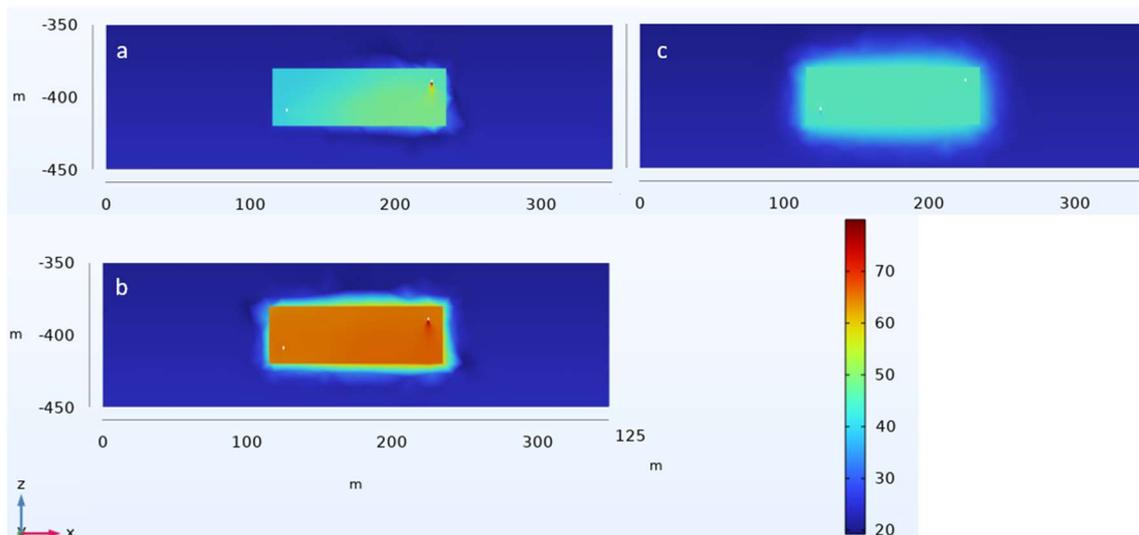

Figure 5. Base case simulation results for temperature after a) 10 days of loading, b) 90 days of loading (end of loading phase) and c) end of unloading (after 90 days rest and 90 days unloading).
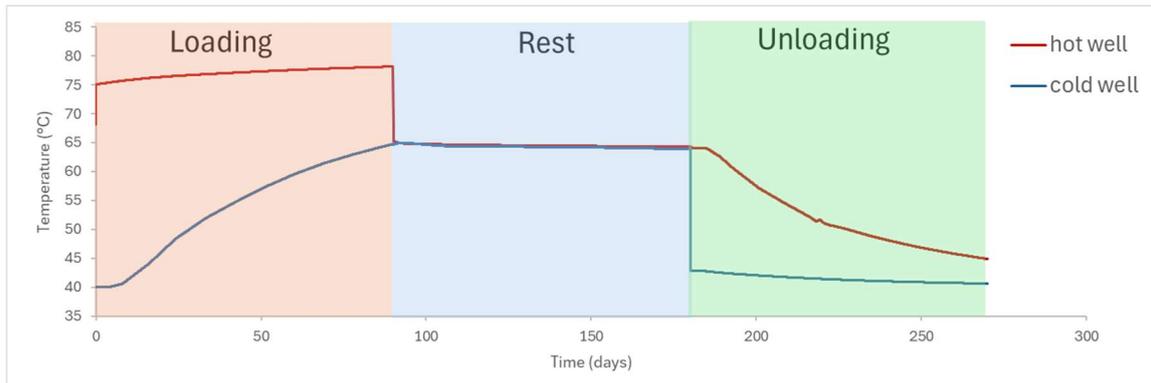
Figure 6. Base case simulated temperature evolution (in °C) at the hot and cold well for the loading, rest and unloading phases of the first operational year. The temperature at the hot well during loading is not constant at 80°C but goes up from 75 to 80°C and is the result of turbulent kinetic energy at fixed flow rate. The same is true for the temperature at the cold well during unloading which goes down from 43 to ~40,6°C.

The thermal efficiency is computed by the energy stored divided by the energy produced:

$$Thermal\ efficiency = \frac{Energy\ (out)}{Energy\ (in)}$$

In contrast to ATES systems, the energy in and out of the system is based on heat fluxes rather than temperature differences between the wells, as heat transfer is more complex in turbulent than in laminar flow:

$$Energy(in)_{loading} = \left(\sum_{t=90\ days}^{t=0} Total\ heat\ flux\ hot\ well - Total\ heat\ flux\ cold\ well \right)$$

$$Energy(out)_{unloading} = \left(\sum_{t=270\ days}^{t=180\ days} Total\ heat\ flux\ hot\ well - Total\ heat\ flux\ cold\ well \right)$$

With total heat flux being the sum of convective and conductive heat flux (W/m^2), which are both significant in turbulent flow, integrated over the inlet/outlet area of the wells.

For the base case scenario, the total energy stored is 8.632 MWh, the total energy retrieved is 4.046 MWh. This gives a thermal efficiency of 47% for the first operational year.

Several sensitivity scenarios were simulated:
- A scenario with full insulation by the salt (closed boundaries at the cavern wall to evaluate the heat loss to the salt and to represent longer time scales)
- A scenario without a rest phase (loading is instantaneously followed by unloading)
- A scenario with an initial temperature in the cavern of 20°C to represent a first operational cycle without pre-heating.
- A scenario with flow rate of 32 kg/s instead of 48 kg/s.

Figure 7 and Figure 8 shows the temperature results and Table 5 the efficiency and energy in and out for the base case scenario and sensitivity scenarios.
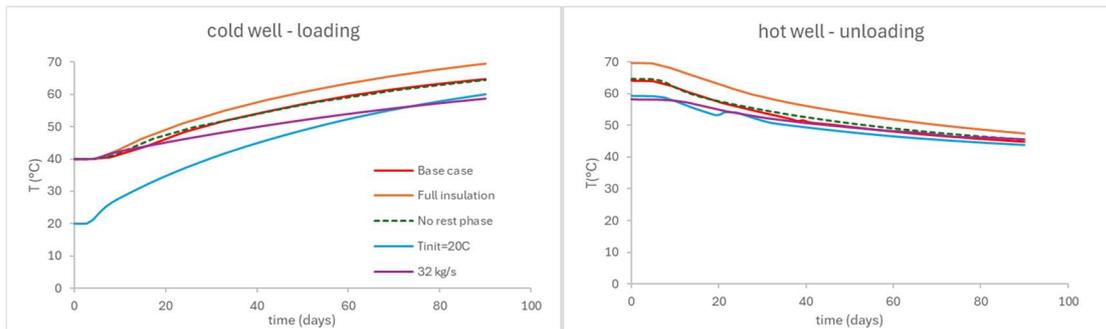
Figure 7. Temperature evolution in the cold well during loading and hot well during unloading for the five different scenarios.
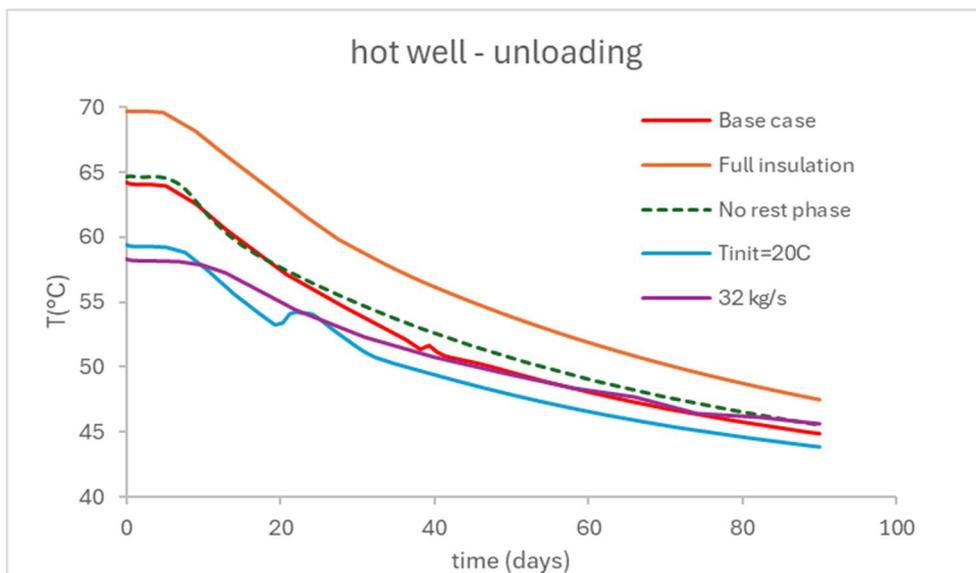

Figure 8. Same figure for temperature in the hot well during unloading as previous figure but with adapted scale for the y-axis. The bumps for the base case and initial temperature of 20°C are due to numerical issues.

The scenario with full insulation shows a faster temperature increase at the cold well during loading, due to the absence of heat loss to the salt close to the hot well. This results in a slightly lower amount of energy stored. As there is no heat loss during the rest phase, the starting temperature during unloading at the hot well is about equal to the final temperature at the cold well during loading, and is roughly 5 °C higher than in the base case (Figure 8). The temperature remains higher during the entire unloading phase, resulting in a higher amount of energy produced (~7 GWh) and an efficiency of 72%. Hence, the heat loss to the salt plays a significant role in the storage efficiency, but is expected to go down in subsequent years, similar to storage in ATES systems.

Because of the high heat loss during the rest phase it would be beneficial to have as little time as possible between loading and unloading. The scenario without rest phase shows that the production temperature is initially similar to the base case, as most heat loss seems to occur during the loading phase. However, over time the production temperature remains higher, leading to a higher efficiency of 50% instead of 47%.

For the scenario with an initial temperature in the cavern of 20°C, with a return temperature of 40 °C (equal to the base case), the amount of energy that is stored is significantly higher (11,7 GWh) due to the higher delta T. But the temperature at the end of loading, and hence at beginning of unloading, is low (~59,4°C) (Figure 8). The total energy retrieved is much lower and the resulting efficiency is 28%. This scenario would be representative for the first operational year in case there is no preheating of the brine in the system. Two additional operational years were simulated. The total energy in goes down and the energy out goes up. As a result the efficiency goes up to 63 and 72% respectively (Table 6).

A lower flow rate of 32 kg/s results in less energy stored, lower temperatures, lower energy produced and very low efficiency (37%). The starting temperature during unloading is 58°C (Figure 8). In these simulations, where the loading and unloading phases are (only) three months each, a higher flow rate is then obviously beneficial for the performance of the system. The higher electricity use by the pumps at higher flow rates then needs to be considered, presenting an optimization challenge.

Table 5. Scenarios run in the sensitivity analysis. In each scenario one of the inputs is changed compared to the basecase.

	Scenario	Energy in (MWh)	Energy out (MWh)	Efficiency (-)
1	**Base scenario**	8.632	4.046	0,47
2	**With full insulation**	7.541	5.506	0,73
3	**No rest phase**	8.618	4.301	0,50
4	**Initial temperature 20°C**	11.730	3.278	0,28
5	**Flow rate 32 kg/s**	6.565	2.434	0,37

Table 6. Simulation results for the three operational years for scenario 4.

	First year			second year			third year		
Scenario	Energy in (MWh)	Energy out (MWh)	Efficiency (-)	Energy in (MWh)	Energy out (MWh)	Efficiency (-)	Energy in (MWh)	Energy out (MWh)	Efficiency (-)
4. Initial temperature 20°C	11.730	3.278	0,28	7.321	4.626	0,63	6.816	4.921	0,72

5.2   Geomechanical safety

The DIANA geomechanical simulation results will be discussed with respect to the safety criteria as described in Section 3.3 for three temperature scenarios (Table 7), as salt creep depends highly on temperature. The extreme storage temperature of 100 °C was chosen to see if there is a threshold at the upper range of potential storage temperatures relevant for the Netherlands.

Table 7. Scenarios for geomechanical simulations.

Scenario	Temperature levels (injection hot well/injection warm well)
Base case	80/40°C
60/20	60/20°C
100/40	100/40°C

The simulation results, as shown in Figure 9, predict that the subsidence at surface level is approximately the same for the three temperature scenarios; ~1.1 to 1.2 cm at the end of the 29 operational years including salt mining, rest (equilibration) and 10 years of cyclic heat storage. This is well below the (roughly assumed) maximum of 25 cm for the lifetime of an operation (see section 3.3). For the 10 operational years of heat storage, the subsidence is approximately 6 mm, this is on average 0.6 mm/yr. The vertical displacement *at the top (subsidence) and bottom (uplift) of the cavern* is, as expected, largest for the 40 - 100°C scenario with subsidence of 22 cm at the top and uplift of 22 cm at the bottom. Displacement is smallest for the 20 - 60°C scenario with a total subsidence and uplift of ~16 cm for top and bottom of the cavern respectively.
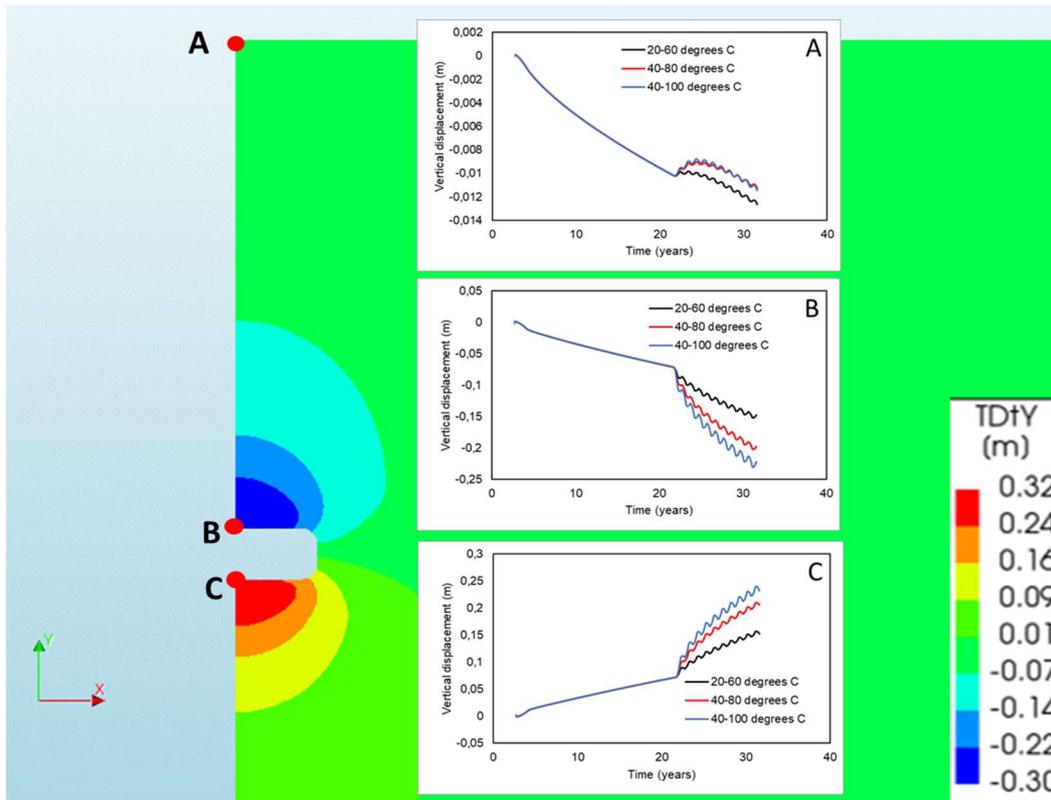

Figure 9. Vertical sediment displacement for the three temperature scenarios at position A (ground level), B (top of cavern) and C (bottom of cavern). Negative displacement represents subsidence, positive displacement represents uplift. The initial uplift at ground level during the first few cycles of heat storage are related to expansion at increasing temperature. Subsequent subsidence is due to underpressure within the cavern.

6 Discussion

The concept of heat storage in salt caverns is partially similar to heat storage in aquifers, with a hot and cold well in a single water(bearing) volume and reversed flow over the seasons. The key difference lies in the flow dynamics of an open space filled with brine, compared to those of a porous medium. Turbulent flow within the cavern results in quick mixing of the hot and cold water and a fast breakthrough at the producing well during loading and unloading. During loading, the temperature of the production water at the cold well increases quickly, thereby reducing the delta T with the hot well and hence the amount of energy that is added to the water for storage. During the rest phase, the temperature in the cavern is quickly homogenized and part of the heat is lost to the surrounding salt. The starting temperature during unloading is therefore well below the storage temperature. The system would benefit from either a high flow rate or a longer loading phase to obtain a high homogeneous temperature in the cavern prior to unloading. Yet, a cavern temperature close to the storage temperature would be unrealistic to achieve, as the temperature difference between hot and cold well goes down during loading, and above a threshold, the electricity required for pumping would outweigh the benefits of the small amounts of energy that can be added to the production water. The same is true for the unloading phase, when the temperature of the water at the hot well reduces to values close to the return temperature in the cold well. By then, only a very limited amount of heat can be extracted for use, and the temperature may be too low for the specific heat network. A cut off temperature would have to be defined. Optimal loading and unloading conditions are case specific. The system also benefits from short or no rest phases, and the application to shorter term heat storage (i.e. weeks) could be interesting to further evaluate. Due to the turbulent flow, the system efficiency is probably more sensitive to variations in conditions then for HT-ATES systems.

In Twente, the prognosis is that 11.456 TJ/yr will be supplied via the regional heat network in 2030, of which 6.620 TJ will be used for heating of houses and buildings. This is equal to ~1.839 GWh. The amount of heat that could be produced from the cavern, based on the first order simulations performed in this study, would be roughly 3 to 4 GWh with a thermal efficiency of 28-50% in the first operational year, depending on whether pre-heating of the brine was considered, and the duration of a rest phase. In subsequent operational years, both the heat output and the efficiency increase. Heat production could increase to >6 GWh with efficiencies to 73% in the subsequent operational years, for which the scenario with full insulation by the surrounding salt is considered representative. Optimization of the system with higher flow rates and/or longer loading and unloading phases could result in somewhat higher values, but it would still be a fraction of the total heat demand of the network. Yet, these estimates are similar to the first operational years of the HT-ATES in Middenmeer from which 2.470 MWh was delivered to greenhouses in year 1, 4.240 in year 2 and 6.490 MWh in year 3 (Drijver, 2024). Thermal efficiencies were respectively 28%, 41% and 44%. The system was designed for a maximum heat delivery of 20.000 MWh (20 GWh) but this power output will not be reached as storage volumes are smaller in practice and heat losses experienced during hot water injection and production were not accounted for. Note that in our simulations heat losses during transport in the wells were also not accounted for.

The evaluation by Ekwadraat (2019) resulted in a heat contribution of 66.000 GJ (18.333 MWh) based on a storage volume of 500.000 m^3 and temperature levels of 75°C and 40°C for respectively storage and return. If we scale this to our volume of 200.000 m^3, this would be 66.000 x 0,4 = 26.400 GJ, which equals 7.334 MWh. This is slightly higher than the high end of our simulations,

even though the storage temperature is 5°C higher in our study, but represents a similar order of magnitude. A key difference in the approach is that Ekwadraat assumed that the entire storage volume can be increased in temperature from the initial value to the desired storage value, and that the same amount of energy can be extracted, thereby not considering the fact that fast mixing of hot and warm water within the cavern will not allow an overall cavern temperature close to the storage temperature, as explained above.

This study shows that salt cavern heat storage is possible from thermal and geomechanical point of view. Yet, the impact of turbulent flow and fast mixing of hot and warm water during charging and discharging on temperature levels and heat supply needs consideration. It implies the application of a cut off temperature, both during loading and unloading, which is required to prevent unnecessary electricity use for pumping of the water when the temperature difference between hot and cold well becomes too small. In a next step, the thermal simulations could be improved, and heat output can be optimized if more detailed information regarding the heat network (i.e. temperature levels) and available salt caverns (i.e. dimensions and well data) is available. The COMSOL model, as developed within this study, could be used for this purpose. The details, which are required for more dedicated thermal simulations have not been provided for this study.

In a follow-up study, the next steps could be:
- Evaluate well design, configuration and materials for available caverns in the region
- Assess dimensions of caverns at the potential storage sites
- Evaluate temperature of the heat source
- Evaluate required supply and return temperatures of the heat network
- Evaluate annual supply and demand profiles
- Determine the cut off temperature during discharging
- Techno-economic assessment, including optimization of the cut off temperature at the warm well during charging

7 References

Bonanos, A.M. and Votyakov, E.V. (2016). Sensitivity analysis for thermocline thermal storage tank design. *Renewable Energy 99, 764-771.*

Dinkelman, D., van Bergen, F. and Veldkamp, J.G. (2020). WINDOW Deliverable B2 Potentieel en toepassingscondities – Geologisch model, temperatuurmodel voor de ondiepe ondergrond en potentieelkaarten voor HTO in Nederland. TNO 2020 R11686

Drijver, B. (2024). HTO Middenmeer – Thermisch opslagrendement en gerelateerde effecten (eerste 3 cycli). *Bijeenkomst Kenniscentrum Bodemenergie – Warmteopslag in de ondergrond, 12 juni 2024.*

Ekwadraat (2019). Hergebruik van ondergrondse cavernes voor warmtetoepassingen. [Link to document](.).

Karim, A., Burnett, A., & Fawzia, S. (2018). Investigation of stratified thermal storage tank performance for heating and cooling applications. *Energies, 11, 1049.* https://doi.org/10.3390/en11051049

Mollema, D. (2011). Underground storage of Diesel fuel oil in Salt Caverns Introduction *About AkzoNobel AkzoNobel Hengelo.*

Njoku, H. O., Ekechukwu, O. V., & Onyegegbu, S. O. (2014). Analysis of stratified thermal storage systems: An overview. *Heat and Mass Transfer 50, 1017–1030.* https://doi.org/10.1007/s00231-014-1302-8

Park, D., Kom, H-M., Ryu, D-W., Choi, B-H., Sunwoo, C. and Han, K-C (2013). The effect of aspect ratio on the thermal stratification and heat loss in rock caverns for underground thermal energy storage. *International Journal of Rock Mechanics & Mining Sciences 64, 201-209.*

Susan, M. (2019). Exploring the Energy Storage Capacity of Salt Caverns in the Netherlands. *EES-2019-372.*

Appendix A

Mesh Generation

In CFD modeling, the volume is divided into numerous small cells or elements, which collectively form a mesh. Each cell in this mesh corresponds to a specific region where the flow is analyzed. The flow physics are then modeled by applying mathematical equations to each of these cells. Ensuring that the mesh is of high quality is vital for obtaining accurate results and maintaining the stability of the numerical calculations.

The worst non-inverting deformation of a mesh element is skewing, where angles deviate significantly from 90°, leading to reduced local accuracy and making equations harder to solve. Skewed elements often occur in boundary layer meshes, curved geometries, or when transitioning between different element types. Skewness is used to detect such distortions, and while there's no strict quality threshold, values below 0.01 should be avoided.

In CFD problems, the mesh contains the shape functions that represent the flow and pressure fields. Sharp gradients in these fields necessitate a denser mesh in specific areas to accurately capture the details. If these gradients are not adequately resolved, the numerical discretization scheme, such as stabilization or upwinding, may dissipate them, leading to reduced accuracy or even causing oscillations and divergence. A smart approach to meshing involves strategically increasing mesh density where higher gradients are expected, rather than uniformly refining the mesh across the entire domain. A skilled fluid mechanics expert can anticipate these critical areas and apply finer meshing accordingly.
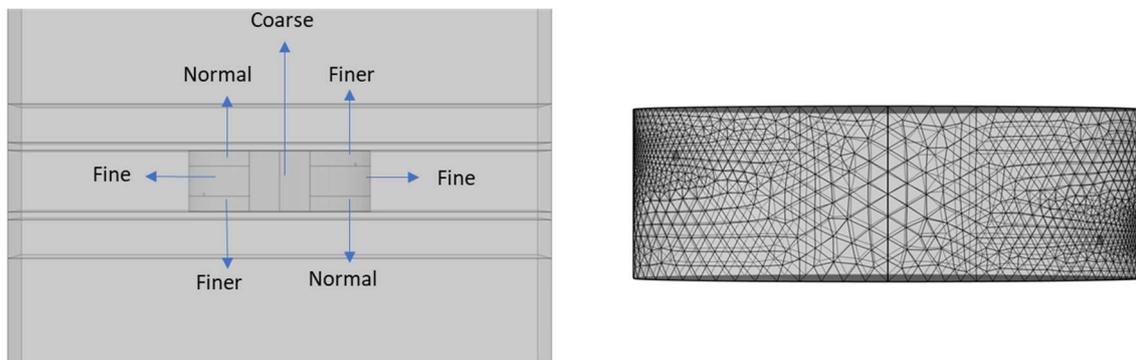

Figure 10. Mesh configuration showing varying densities, with finer mesh near the hot and warm wells to accurately capture high gradients, and coarser mesh in less critical areas for computational efficiency

As shown in Figure 10, the mesh configuration for our CFD simulation is carefully designed to optimize both accuracy and computational efficiency by varying the element sizes across different regions of the domain. The mesh is made finer near the hot well and warm well, where temperature and pressure gradients are higher, with element sizes ranging from 1.18 m to 10.9 m. This targeted refinement ensures that the mesh can accurately capture the sharp changes in these critical areas, leading to more precise simulations of flow dynamics and heat transfer. A fine mesh setting, with element sizes between 2.96 m and 15.7 m, is used in those parts of the model requiring moderate detail, providing a balance between precision and computational cost. The normal mesh, with element sizes from 5.92 m to 19.8 m, is likely applied in zones where flow features are less critical, offering a reasonable trade-off between accuracy and computational load. Finally, a coarse mesh, with element sizes from 8.87 m to 29.6 m, is used in regions where fine

detail is unnecessary, significantly reducing computational demands. This strategic variation in mesh density ensures high accuracy where needed, while effectively managing overall computational resources. Despite a large number of elements, the minimum element quality of 0.141 indicates that the mesh maintains a reasonable standard, contributing to reliable and stable simulation results.

In conclusion, this carefully designed mesh setup is crucial for ensuring the accuracy and reliability of the CFD simulations by precisely capturing the critical flow dynamics and thermal gradients within the salt cavern. The strategic variation in mesh density allows for a detailed and computationally efficient simulation, which is essential for obtaining meaningful results.

Warming^{UP}*GOO*
Geothermie & Opslag Opschaling

Adres
Princetonlaan 6
3584 CB Utrecht

Postadres
Postbus 80015
3508 TA Utrecht

Telefoon
088 866 42 56

E-mail
contact@warmingup.info

Website
www.warmingup.info